ISBN: 978-3-95450-247-9 ISSN: 2673-5490 doi: 10.18429/JACoW-IPAC2024-MOPR69

HIGHLY CHARGED Mg ION PRODUCTION USING LASER ABLATION ION SOURCE AT BROOKHAVEN NATIONAL LABORATORY*

M. Horana Gamage[1†], A. Cannavo[2], G. Garty[1], S. Ikeda[2],
T. Kanesue[2], S. Kondrashev[2], M. Okamura[2]
[1] Columbia University, New York, NY, USA
[2] Brookhaven National Laboratory, Upton, NY, USA

Abstract

This study explores the generation of highly charged Mg ions within an ultra-high intensity heavy ion source, integrating laser ablation ion source (LIS) technology with an unique beam injection method known as Direct Plasma Injection Scheme (DPIS). A Q-switched Nd:YAG (Thales SAGA 230/10) laser is employed to ablate a Mg target, leading to the generation of a pulsed high-density plasma. The ions are then extracted and injected into the RFQ, where they undergo RFQ acceleration. After ion acceleration, the current transformer (CT) recorded a total beam current exceeding 30 mA. Mg^{9+} ion beam currents exceeded 20 mA, achieving a maximum of 23 mA with $\sim 10^{10}$ particles recorded by the Faraday cup (FC) after analyzing dipole magnet. The results underscore the potential for improving heavy ion beam production, with implications for various scientific domains and medical applications, particularly in particle therapy.

INTRODUCTION

The production of heavy ion beam currents plays an important role in numerous scientific fields, including nuclear physics, materials science, astrophysics, and medical physics [1, 2]. Over the past few decades, there has been a growing interest in the utilization of heavy ion beams for particle therapy [3–6]. Three predominant techniques are commonly employed in the production of heavy ion beams: electron beam ion sources (EBIS), laser ion sources (LIS), and electron cyclotron resonance (ECR) [7, 8]. The introduction of the direct plasma injection scheme (DPIS) by Dr. Okamura has led to the rise of the combination of laser ablation source and RFQ accelerator as a promising approach for generating intense heavy ion beam [9]. We explore the potential of employing a laser ablation ion source coupled with an RFQ accelerator at Brookhaven National Laboratory [10]. Our objective is to examine various solid target materials and optimize the production of intense heavy ion beam. This article details on the production and optimization of intense Mg^{9+} ion beams, aiming to explore their potential utility for medical applications, especially in particle therapy.

EXPERIMENTAL SETUP

Laser Ion Source

Laser ablation is the process of vaporizing and ionizing a target material with an intense laser beam, which results in the formation of a plasma plume. In our experimental setup, we utilize the Nd:YAG Thales SAGA 230/10 laser with a wavelength of 1064 nm. This laser can deliver a maximum of 2.3 J per 10 ns pulse and operates at a frequency of 10 Hz. A laser power density of $\sim 10^{12}$ W/cm^2 is applied to irradiate the target surface material, resulting in the formation of a high-temperature plasma at the focal point. The formed plasma expands normal to the target surface and moves in the direction of radio frequency quadrupole (RFQ) linac. The space charge effect makes it difficult to transport and inject an intense heavy ion beam into the RFQ linac with conventional ion sources. To address this issue, the laser ion source employs a direct plasma injection scheme, wherein the plasma remains unchanged until it reaches the RFQ injection stage. In this technique, the extraction voltage is applied to both the target and the metal housing box of the plasma.

RFQ Accelerator

The RFQ accelerator is a linear accelerator that operates primarily as a front-end accelerator, capable of accelerating charged particles ranging from protons to uranium [11]. The RFQ accelerator serves the dual function of accelerating and focusing the ion beam. This is achieved through the utilization of a transverse electrostatic field for ion focusing and a longitudinal electrostatic field for ion acceleration. The RFQ focusing principle enables high current densities and effective transmission of the beam [12].

At the laser ion source research lab of Brookhaven Laboratory, the RFQ linac accelerates ions from an initial injection energy of $\sim$ 22 keV/n to $\sim$ 204 keV/n during the acceleration process [13]. The nozzle, which enables the release of ions from the ion source into the RFQ, typically maintains within a voltage range of 50 – 60 kV, along with the target and the plasma housing case. This arrangement provides the initial injection energy for the ions that release into the RFQ. The four rod-type RFQ electrodes generate a quadrupole electric field, with the polarity switching as the voltage oscillates between ±33 kV over time at a frequency of 100 MHz.

Apparatus

A 50 mm × 50 mm Mg target with a 3 mm thickness was utilized in the experiment. The high-intensity Nd:YAG laser beam impacts the Mg target, mounted on a two-way movable platform, causing material to be irradiated from the target surface and generating plasma. Plasma formation

* The study at Brookhaven National Laboratory was supported by US DOE, Office of Science, under contract DE-SC0012704.
† mh4482@cumc.columbia.edu

ISBN: 978-3-95450-247-9 ISSN: 2673-5490 doi: 10.18429/JACoW-IPAC2024-MOPR69

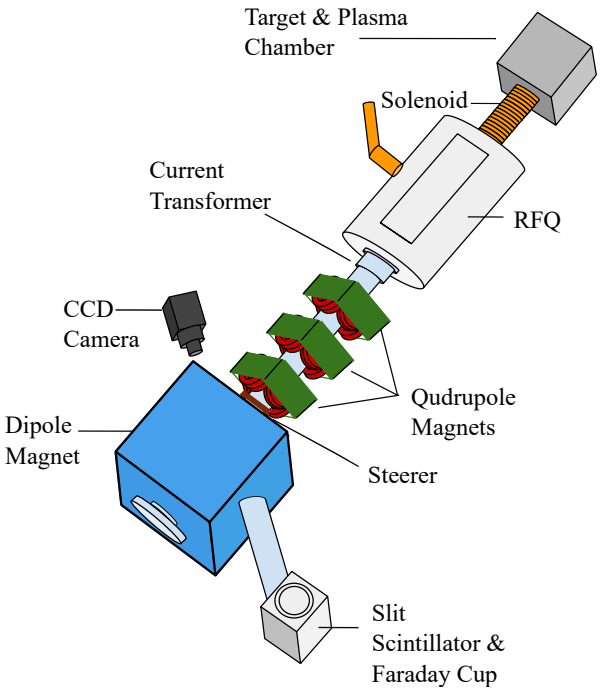

Figure 1: Overview of the experimental setup.

occurs in a 40 cm×40 cm×40 cm plasma chamber (refer to Fig. 1) under a vacuum pressure of 10^{-5} Pa. This chamber also houses the metal casing, which restricts the expansion of the plasma and contains the final focusing lens of the Nd:YAG laser. The casing opens into an aluminum tube inside a 50 cm long solenoid coil. The applied magnetic field (B-field) of the solenoid prevents radial expansion of the moving plasma while allowing axial expansion, facilitating the transport of high-density plasma to the RFQ entrance.

The current transformer (CT) located at the end of the RFQ accelerator measures the entire beam current of assorted charged ions. The mesh installed before the CT to reduce RF noise exhibits a transmission efficiency of 72%. Three quadrupole magnets are sequentially positioned along the beamline following the CT. In a quadrupole B-field, a charged particle beam experiences either a focusing or defocusing force in the transverse direction. Following that, a magnetic steerer is utilized to guide the ion beam. A magnetic dipole is employed in the experimental setup for the efficient separation of ions based on their charge-to-mass ratios. A dipole magnet generates a uniform B-field over a certain distance, resulting in ions injected into it traveling along a circular trajectory. In our apparatus, the ion beam is deflected at a 45° angle from its initial path. Ions are detected at the end of the beamline via either a scintillator or a Faraday cup (FC), based on the chosen method. A slit positioned in front of the scintillator improves the spatial resolution of the detection system.

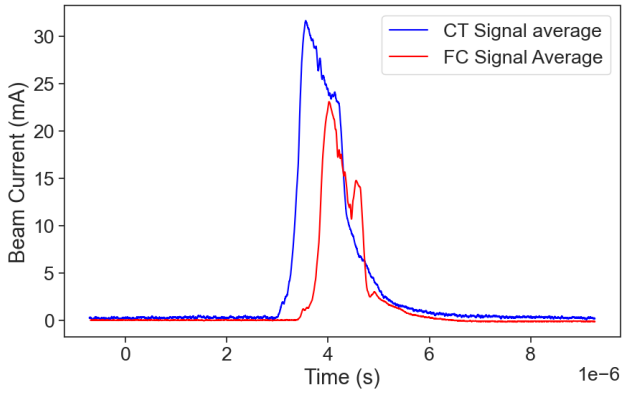

Figure 2: Moving averages of the CT signal (blue) and FC signal (red) representing the Mg^{9+} most beam current yield.

RESULTS AND DISCUSSION

Tremendous progress has been achieved in the beam current of highly charged magnesium atomic ions. In this specific experiment, it has been observed that the beam current of $^{24}Mg^{9+}$ ions exceeded 20 mA. During the experiment, the maximum beam current achieved for Mg^{9+} as measured by the FC signal was 23.07 mA. Table 1 displays the optimized values for the various parameters that were tested in the experiment, which included RFQ power, extraction voltage, solenoid B-field strength, and FC bias voltage. Additionally, other parameters such as B-fields of the three quadrupoles and the steerer were optimized to improve the beam transport to the detectors.

Table 1: Parameters Optimized in the Mg^{9+} Experiement

Parameter	Optimized value
RFQ power	82.7 kW
Solenoid B-field	85 Gauss
Extraction voltage	57 kV
FC bias voltage	-1.5 kV

Figure 2 illustrates the comparison between the CT and the FC signals. The data has been smoothed using a 200-point moving average to enhance readability. The blue signal shows the moving average of the CT signal. It represents the total beam current of multiple highly charged Mg ions. According to the graph, the beam current has crossed the mark of 30 mA. The red signal represents the moving average of the FC signal of Mg^{9+} ions. The FC signal indicates the presence of 9.8×10^9 particles, resulting in a total ion charge of 1.5×10^{-8} C.

The placement of the mesh before the CT lowers ion beam transportation efficiency, resulting in notably reduced signals at both the CT and FC compared to the actual signals. Accounting for the mesh transmission factor, the actual ion beam intensities are 1.39 times greater than the recorded values. In the absence of mesh installation, we anticipate being able to generate more than 32 mA of Mg^{9+} ion beam current at the FC.

ISBN: 978-3-95450-247-9 ISSN: 2673-5490 doi: 10.18429/JACoW-IPAC2024-MOPR69

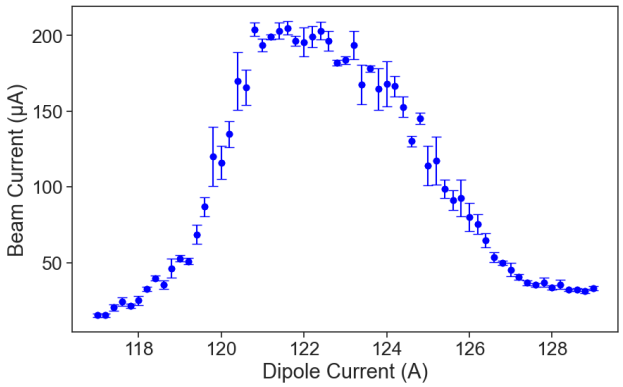

Figure 3: Mg^{9+} beam current (amplified by 25) vs. dipole current, scanned in 0.2 A increments with a 1 mm slit width.

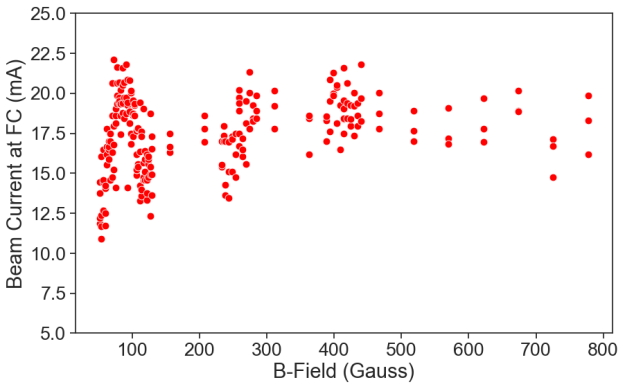

Figure 4: Periodic fluctuations in Mg^{9+} beam current at the FC, correlated with variations in the solenoid B-field.

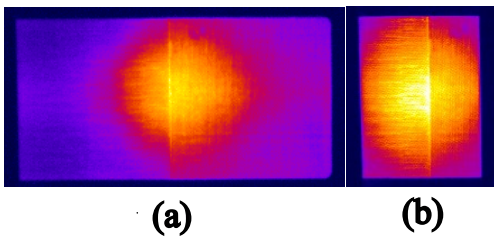

Figure 5: (a) Mg^{9+} beam spot with open slit; (b) Mg^{9+} beam spot with slit width of 25 mm.

One of the raised concerns was the potential presence of additional isotopes of Mg^{9+} in the signals. There are three stable isotopes of Mg ions: ^{24}Mg, ^{25}Mg, and ^{26}Mg, with respective abundances of 78.99%, 10.0%, and 11.01%. In order to address this concern during the experiment, we endeavored to scan the dipole current in small increments of 0.2 A around the maximum ion beam current yield, employing a 1 mm slit. Figure 3 shows the graph of the dipole current scan around 123 A , which represents the optimal dipole current for Mg^{9+}. The graph displays the results of the dipole scan with an amplification factor of 25, aiming to compensate for lower amplitude signals at the FC resulting from the use of a 1 mm slit width.

However, despite these efforts, Mg^{9+} isotope separation could not be achieved. Even if distinct portions are allocated to each isotope based on their abundances, the beam current of ^{24}Mg ions can still surpass 25 mA. In such a scenario, the beam currents for the ^{25}Mg and ^{26}Mg ions would amount to 3.52 mA and 3.2 mA, respectively. We have examined highly charged Al ions, particularly Al^{11+} and Al^{10+}. The dipole scans for these ions displayed a pattern akin to that of Mg^{9+}, indicating that the predominant source of Mg^{9+} ions might be $^{24}Mg^{9+}$, considering that aluminum has only one stable isotope.

Higher B-fields generated by the 50 cm long solenoid are generally favorable for obtaining increased beam currents at the FC following RFQ acceleration. Identifying an optimal lower solenoid B-field range to maximize beam current was challenging in our lab prior to this experiment. The solenoid B-field scan for Mg^{9+} is presented in Fig. 4. The Mg^{9+} beam current fluctuations at the FC exhibit discernible periodicity, with variations in the B-field of the solenoid. Analysis of the graph reveals distinct maxima occurring at approximately 85, 275, and 400 Gauss in B-field strength, corresponding to solenoid currents of 1.7 A, 5.3 A, and 7.7 A, respectively. Continuation of the experiment faces a significant barrier when the solenoid heats up due to prolonged usage beyond 500 Gauss in B-field strength. Hence, identifying the 85 Gauss solenoid field (lower B-field that maximizes Mg^{9+} ion beam current) is crucial for continuous data acquisition and diverse ion experiments.

Modulating the size of the slit aperture induces substantial variations in the ion beam currents. The scintillator images acquired by the CCD are presented in Fig. 5 corresponding to Mg^{9+} ion beam. The Fig. 5(a) illustrates the scenario when the slit aperture is fully opened, while Fig. 5(b) depicts the case when the slit opening is restricted. The ImageJ software was employed for image analysis, specifically for delineating the border of the beam spot. Consequently, this enabled for limiting the opening of the slit to match the diameter of the spot. In this experiment, the beam current for Mg^{9+} decreased from 23.07 mA to 14.51 mA when employing a selective slit width of 25 mm. Excluding the use of the mesh, this beam would measure 20.1 mA.

CONCLUSION

To produce Mg highly charged ions, a high-intensity Nd:YAG laser was utilized, followed by ion acceleration through the RFQ accelerator. The measurement of the intense Mg^{9+} ion beam exceeding 20 mA, with ~10^{10} particles recorded by the FC. The results may contribute to the advancement of ion beam production for diverse scientific applications, including particle therapy.

REFERENCES

[1] J. D. Gillaspy, "Highly charged ions," *Journal of Physics B*, vol. 34, no. 19, pp. R93–R130, Sep. 2001. doi:10.1088/ 0953-4075/34/19/201

ISBN: 978-3-95450-247-9 ISSN: 2673-5490 doi: 10.18429/JACoW-IPAC2024-MOPR69

[2] I. Ahmad and M. Maaza, Ion Beam Applications. 2018. doi:10.5772/intechopen.78966

[3] S. E. Combs and J. Debus, "Treatment with heavy charged particles: Systematic review of clinical data and current clinical (comparative) trials," *Acta Oncologica*, vol. 52, no. 7, pp. 1272–1286, Aug. 2013. doi:10.3109/0284186x.2013.818254

[4] J. S. Loeffler and M. Durante, "Charged particle therapy—optimization, challenges and future directions," *Nature Reviews Clinical Oncology*, vol. 10, no. 7, pp. 411–424, May 2013. doi:10.1038/nrclinonc.2013.79

[5] A. Pompos *et al.*, "National Effort to Re-Establish Heavy Ion Cancer Therapy in the United States," vol. 12, Jun. 2022. doi:10.3389/fonc.2022.880712

[6] O. Jäkel, "Heavy Ion Radiotherapy," *Springer eBooks*, pp. 365–377, Jan. 2006. doi:10.1007/3-540-29999-8_28

[7] A. Lapierre, J. Benitez, M. Okamura, D. Todd, D. Xie, and Y. Sun, "Ion Sources for Production of Highly Charged Ion Beams," 2022. doi:10.48550/arXiv.2205.12873

[8] S. Gammino, "Production of High-Intensity, Highly Charged Ions," *arXiv.org*, 2014, doi:10.5170/CERN-2013-007.123

[9] M. Okamura, T. Katayama, R. A. Jameson, T. Takeuchi, T. Hattori, and H. Kashiwagi, "Scheme for direct plasma injection into an RFQ linac," *Laser and Particle Beams*, vol. 20, no. 3, pp. 451–454, Jul. 2002, doi:10.1017/S0263034602203171.

[10] T. Kanesue and M. Okamura, "Laser ion source activities at Brookhaven National Laboratory," *Radiation Effects and Defects in Solids*, vol. 170, no. 4, pp. 347–354, Apr. 2015, doi:10.1080/10420150.2015.1036427.

[11] C. Zhang, Radio-Frequency Quadrupole Accelerators. *Springer Nature*, 2023, doi:10.1007/978-3-031-40967-7.

[12] M. Vretenar, "The radio-frequency quadrupole," *arXiv.org*, 2013. doi:10.5170/CERN-2013-001.207

[13] M. Okamura *et al.*, "Demonstration of an intense lithium beam for forward-directed pulsed neutron generation," *Scientific Reports*, vol. 12, no. 1, p. 14016, Aug. 2022, doi:10.1038/s41598-022-18270-0